Formation of Carbon Species on Ni(111): Structure and Stability

Sheng-Guang Wang,[†] Xiao-Yuan Liao,[†] Dong-Bo Cao,[†] Yong-Wang Li,[†] Jianguo Wang,[†] and Haijun Jiao*[,†,‡]

State Key Laboratory of Coal Conversion, Institute of Coal Chemistry, Chinese Academy of Sciences, Taiyuan, Shanxi 030001, P. R. China, and Leibniz-Institut für Katalyse e.V. an der Universität Rostock, Albert-Einstein-Strasse 29a, 18059 Rostock, Germany

Received: January 24, 2007; In Final Form: May 14, 2007

The structures and stabilities of a set of carbon species on the Ni(111) surface, as well as the energy barriers of the initial stages of carbon growth, were computed by using density functional theory. It was found that the stability is on the order of graphitic monolayer > C in Ni bulk > carbon chain > small cluster > atomic carbon. The formation of adsorbed graphitic monolayer is most preferred on Ni(111) thermodynamically. The adsorbed carbon atoms exist at the coverage of 0.25 and 0.5 monolayer, and they reconstruct Ni(111) at the coverage of 0.75 and 1 monolayer. The reconstruction will be interesting for self-assembly of surface structures and needs experimental confirmation. The adsorbed C_2 and C_3 carbon clusters on Ni(111) have linear structures, in which the terminal carbons prefer occupying 3-fold hollow sites. In the stable adsorbed C_3 cluster, the middle carbon atom occupies a top site. The linear C_4 cluster and the branched C_4 cluster have very similar stability. Like the adsorbed graphitic monolayer, the branched C_4 cluster occupies similar surface sites, and this implies a simple carbon growth mechanism. On the basis of the computed energy barriers, the lateral transfer and clustering of carbon is favored kinetically, while the carbon atoms sinking into the Ni bulk have high energy barriers. During the adsorption processes, electrons transfer from the Ni surfaces to the adsorbed carbon species, while the spin densities of the adsorbed carbon species and the Ni surfaces decrease.

1. Introduction

Because of their good catalytic activity Ni-based catalysts are widely used in chemical processes such as steam reforming, catalytic partial oxidation, and dry reforming of methane. Compared to Pt, Pd, and Rh, the low price makes Ni a very attractive catalyst material,[1] but carbon deposition is especially severe for nickel-based catalysts and usually deactivates the catalysts.[2−7] There are two main carbon phases identified with Ni-based catalysts:[8,9] (1) as reaction intermediates in the active phase, and (2) deactivating the catalysts in the inactive phase. The adsorbed carbon atoms are usually produced by the dissociation of the adsorbed hydrocarbons or carbon monoxide in the above-mentioned chemical reactions as well as the adsorption of free atomic carbon in some other processes. The inactive phase is the so-called carbon deposition, which forms a graphitic monolayer or amorphous carbon filament. The sinking of atomic carbon into a Ni particle is considered as the first step for the formation of amorphous carbon filament.

Generally the poisoning of a catalyst can be temporary, which means that the catalyst can be reactivated and recovered by performing some treatments, or it can be permanent if the catalyst cannot be reactivated. The graphitic carbon layer on a transition metal surface produces permanent poisoning. Therefore, to keep a catalyst active, it is very helpful to know the deactivation mechanism during the growth of carbon species. Especially, studies of the initial stage of carbon growth are useful, because it is still possible to recover the catalysts and restrain the further growth of carbon clusters, while the catalysts with graphite and carbon filament formed are already permanently poisoned.[9]

Experimentally, it is very difficult to characterize the structures and the properties of the Ni surfaces covered by small carbon clusters, and only a few theoretical studies were focused on this topic. Kalibaeva et al. calculated the poisoning of a nickel surface due to carbon by using free energy density functional theory,[9] and the stable state of the nickel/carbon surface was found to be either a clean nickel surface or a fully carbon-covered nickel surface with a graphitic configuration. The relative stability of the two states depends on the temperature and partial pressure of the carbon gas. At fixed nominal carbon coverage, the most stable configurations are those forming carbon clusters.

In the present paper, theoretical calculations are performed on the adsorption of carbon species on the Ni(111) surface. Compared to Kalibaeva et al.'s work, many new results are obtained on the aspects of the surface reconstruction of Ni-(111) by the adsorbed carbon atoms and the stability of the small carbon clusters. In Section 3.1, the adsorbed atomic carbons on Ni(111) are calculated, and surface reconstruction is found at the coverage of 0.75 and 1 monolayer (ML). In Section 3.2, the adsorbed small carbon clusters (C_2∼C_4) are calculated, and new stable structures for C_3 and C_4 clusters are found and compared to Kalibaeva et al.'s result. Hereby we propose a very different growth mechanism of the adsorbed graphitic monolayer. The calculation on the other carbon species is presented in Section 3.3, and a comparison of all types of carbon species is performed. In Section 3.4, the energy barriers of the initial stage of carbon growth on the Ni(111) surfaces are calculated

* Corresponding author. E-mail: haijun.jiao@catalysis.de.
† Chinese Academy of Sciences.
‡ Universität Rostock.

10.1021/jp070608v CCC: $37.00
Published on Web 07/04/2007

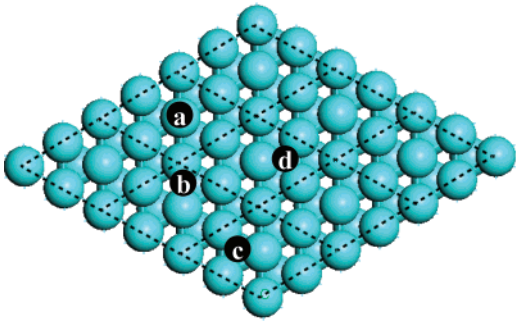

Figure 1. Top view of Ni(111): (a) top (tp) site, (b) bridge (br) site, (c) hexagonal-close-packed (hcp) site, and (d) face-centered cubic (fcc) site.

and analyzed. In Section 3.5, the electronic properties, such as the charge transfer and the changes of the spin states, are analyzed.

2. Methods and Models

Adsorption of carbon clusters on Ni(111) was computed at the level of density functional theory by using the Cambridge Sequential Total Energy Package (CASTEP).[10] The exchange correlation energy was described with the Perdew-Burke-Ernzerhof form using the generalized gradient approximation (GGA-PBE[11]). Ionic cores were described by ultrasoft pseudopotential,[12] and the Kohn−Sham one-electron states were expanded in a plane wave basis set up to 270 eV. A Fermi smearing of 0.1 eV was utilized. Brillouin zone integration was approximated by a sum over special *k*-points ($4 \times 4 \times 1$) chosen using the Monhorst−Pack scheme.[13] Spin polarization was also used to calculate the energies and structural parameters of all models. Without counting the adsorbates, the vacuum between the slabs was set to span the range of 12 Å for the slabs without significant interaction. The convergence criteria for structure optimization and energy calculation were 1.0×10^{-6} eV/atom for SCF, 2.0×10^{-5} eV/atom for energy, 0.05 eV/Å for maximum force, and 2.0×10^{-3} Å for maximum displacement.

The three-layered models were employed. In our calculations, the nickel atoms in the bottom layer were fixed in their bulk positions, while those in the top and second layers were allowed to relax (1 Ni/2 Ni). The validity of these models was testified and benchmarked in previous papers.[14,15] As shown in Figure 1, the p(2×2) unit cell was used, which was widely used in the previous theoretical investigations on the molecule chemisorptions on transition metal surfaces.[14−18]

The adsorption energy of the adsorbed C_n species was defined as $E_{ads} = E(C_n/slab) - [nE(C) + E(slab)]$, where $E(C_n/slab)$ is the total energy of the slab with the adsorbed C_n on the surface, $E(C)$ is the total energy of the free carbon atom, and $E(slab)$ is the total energy of the bare slab of the surface. Therefore, a negative E_{ads} means exothermic adsorption. The adsorption energy relative to graphitic monolayer is calculated by E_{ads}(graphitic) $= E$(graphitic/slab) $- [E$(graphitic) $+ E$(slab)], where E(graphitic/slab) is the total energy of the slab with the adsorbed graphitic monolayer, and E(graphitic) is the total energy of free graphitic monolayer. The average adsorption energy per atomic carbon was defined as $E_{ads}(C) = E_{ads}/n$ and was used for direct comparison.

The transition states (TS) are located by using the complete LST/QST method.[19] First, the linear synchronous transit (LST) maximization was performed, followed by an energy minimization in directions conjugate to the reaction pathway. The TS approximation obtained in that way is used to perform quadratic synchronous transit (QST) maximization. From that point, another conjugate gradient minimization is performed. The cycle is repeated until a stationary point is located. The convergence criterion for transition state calculations was set to a root-mean-square forces on atom tolerance of 0.25 eV/Å. Due to the technical limitation of CASTEP, the computed transition states could not be validated by frequency calculation. The LST/QST method is numerically approximated, but qualitatively accurate, for the surface reactions with simple processes. As the reactions computed in the present paper are only for the transfer of one atom, we believe that the results from the LST/QST method are reliable.

TABLE 1: Average Adsorption Energies (E_{ads}(C), eV) per Carbon Atom of the Adsorbed Carbon Atoms

coverage (ML)	site	E_{ads}(C)
0.25	fcc	−7.06
	hcp	−7.09
0.50	fcc+hcp	−6.24
	2fcc	−6.22
0.75		−6.74
1.00		−6.18

3. Results and Discussion

3.1. Atomic Carbon. The adsorption of atomic carbon was first calculated at the different coverages. The computed adsorption energies are shown in Table 1, and the optimized structures are shown in Figures 2 and 3. Carbon atoms prefer binding at the 3-fold hollow sites, i.e., the face-centered cubic (fcc) and hexagonal-close-packed (hcp) sites of the Ni(111) surface.[15]

The adsorption at the coverage of 0.25 ML corresponds to one carbon atom in one p(2×2) unit cell. The adsorption energies on the fcc and hcp sites (−7.06 vs −7.09 eV) are very close. Therefore, the difference between the two 3-fold hollow sites was not considered in the subsequent calculations.

At 0.5 ML coverage, two relative locations were calculated (Figure 2). The E_{ads}(C) values are −6.24 and −6.22 eV for C (fcc + hcp) and C (2fcc), respectively, indicating that no apparent preference exists for the two computed co-adsorption modes. Compared to those at 0.25 ML, the adsorption energies are less negative at 0.5 ML. The nearest C−C distances are 2.884 and 2.579 Å for C (fcc+hcp) and C (2fcc), respectively. They are much shorter than 5.012 Å in C (hcp) and C (fcc).

The adsorbed atomic carbons at 0.75 ML reconstruct the Ni-(111) surface (Figure 3). In the initial structure, the carbon atoms were put homogeneously on the fcc sites. During the geometry optimization, the three C atoms, which are near to each other, moved closely and formed a triangular C_3 cluster (C−C distances are 1.509, 1.510, and 1.513 Å). At the same time, the surface Ni atoms connecting the corner of the C_3 clusters moved out of the Ni(111) surface. These drawn-out Ni atoms bind with the C_3 clusters (Ni−C distances are 2.035, 2.035, and 2.043 Å). As a consequence, the Ni(111) surface is deformed and reconstructed, the surface vacancies are formed on the Ni-(111), and the adsorbed layer changes to the net form composed of the C_3 three-membered rings and the Ni_3C_6 nine-membered rings.

A similar reconstruction was found for adsorbed atomic carbons at 1 ML. In the initial structure, four fcc sites were occupied by four C atoms, respectively. After the reconstruction, the adsorbed net structure composed of the C_3 three-membered rings and the Ni_3C_6 nine-membered rings is formed, and the

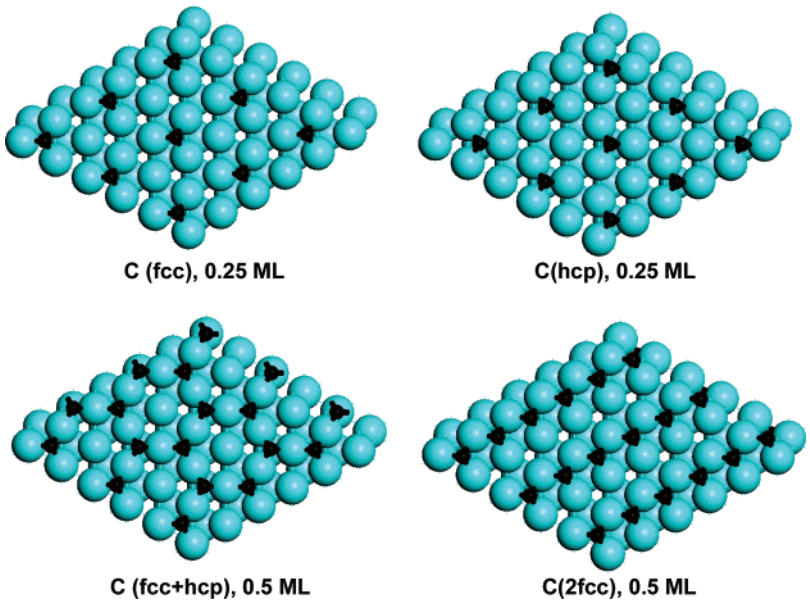

Figure 2. Top view of the adsorbed carbon atoms on the Ni(111) surface at 0.25 and 0.5 ML.

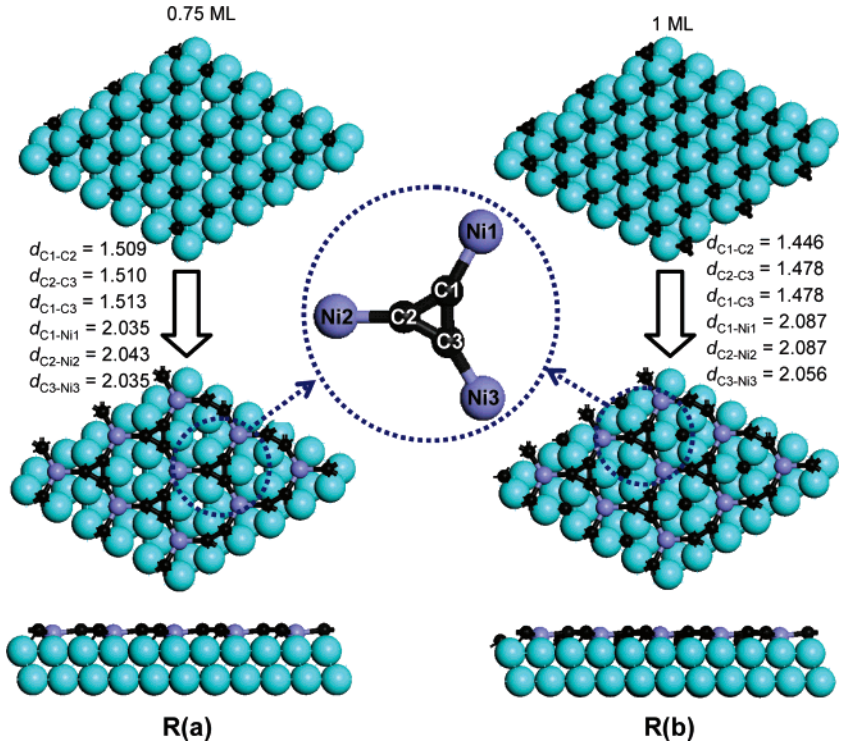

Figure 3. Reconstructed structures of the Ni(111) surface caused by the adsorbed atomic carbons at 0.75 and 1 ML. The purple balls with intermediate size represent the Ni atoms outside the Ni(111) surface.

3-fold hollow site (fcc) in the center of the Ni_3C_6 nine-membered rings is occupied by the fourth C atom. This C atom is near to the formed vacancies. Compared to the situation at 0.75 ML, the C−Ni distances at 1 ML are elongated, and the C−C distances are shortened by the carbon atom in the center of the Ni_3C_6 ring. It indicates the increase of the radius of the Ni_3C_6 ring and the decrease of the radius of the C_3 ring.

The spontaneous formation of the net structure in three-membered C_3 rings and nine-membered Ni_3C_6 rings could be interesting for the self-assembly of surface structures. It implies that we could synthesize the net structure by self-assembly if we can prepare the dispersed carbon atoms at a coverage of 0.75 and 1 ML on Ni(111). This needs experimental confirmation.

The computed E_{ads}(C) at 0.75 and 1 ML are −6.74 and −6.18 eV, respectively. It should be noted that the higher coverage induces less negative adsorption energy. Nevertheless, the values at 0.75 and 1 ML are more negative than that at 0.5 ML, and these changes are caused by both the adsorption and the reconstruction. Therefore, the reconstruction stabilized the surface. Since Kalibaeva et al.[9] did not calculate the situation at coverage higher than 0.5 ML, it is not possible for direct comparison.

The reconstruction of the Ni surface was tested by using the six-layered Ni surface models with two bottom layers fixed in their bulk position (2 Ni/4 Ni), and the same reconstructions were found. At a coverage of 0.75 ML, the C−C distances are 1.507, 1.507, and 1.519 Å, while the Ni−C distances are 2.036,

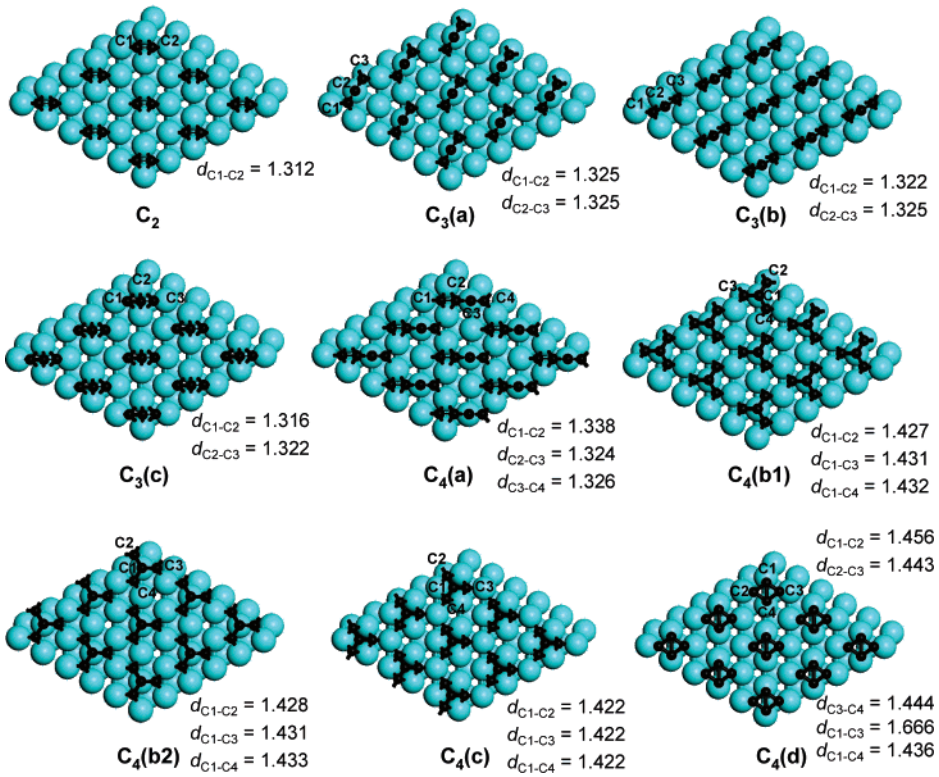

Figure 4. Top view of the adsorbed carbon clusters (C_2∼C_4) on the Ni(111) surface.

TABLE 2: Total Adsorption Energies (E_{ads}, eV) of the Adsorbed Carbon Clusters, and the Average Values (E_{ads}(C), eV) per Carbon Atom

species	E_{ads}	E_{ads}(C)
C_2	−14.27	−7.13
C_3(a)	−21.43	−7.14
C_3(b)	−21.03	−7.01
C_3(c)	−20.41	−6.80
C_4(a)	−27.41	−6.85
C_4(b1)	−27.27	−6.82
C_4(b2)	−27.27	−6.82
C_4(c)	−26.72	−6.68
C_4(d)	−25.09	−6.27

2.036, and 2.045 Å. At a coverage of 1 ML, the C−C distances are 1.469, 1.470, and 1.470 Å, while the Ni−C distances are 2.089, 2.094, and 2.096 Å. The computed bond lengths are close to those computed by three-layered models. The computed E_{ads}(C) at 0.75 and 1 ML are −6.56 and −6.04 eV, which are close to those by three-layered models (−6.74 and −6.18 eV).

3.2. Small Carbon Clusters. The adsorption of small carbon clusters was calculated to cast light on the initial stage of the carbon growth on the Ni(111) surface. The optimized structures are shown in Figure 4 and the computed adsorption energies are listed in Table 2.

For the adsorbed C_2 cluster, the two carbon atoms occupy a fcc site and a hcp site, respectively. The E_{ads}(C) of C_2 is −7.13 eV, which is more negative than those (−6.24 and −6.22 eV) of the adsorbed atomic carbons at 0.5 ML. It indicates that the stability of the adsorbed carbon cluster is higher than the adsorbed atomic carbon at the same coverage. The computed C−C distance of the adsorbed C_2 cluster is 1.312 Å.

Many initial structures of the adsorbed C_3 clusters were calculated, but only three stable structures were obtained, C_3(a∼c), where three carbon atoms are put into a p(2 × 2) unit cell, corresponding to the coverage of 0.75 ML. For the most stable C_3(a) cluster, the two terminal carbons adsorb on a fcc and a hcp site, respectively; the middle carbon atom adsorbs on a top site of the Ni(111) surface. The C−C distances of C_3(a) are both 1.325 Å. The E_{ads}(C) is −7.14 eV, which is more negative than that of the reconstructed structure at 0.75 ML. It indicates that the carbon cluster is preferred to form energetically.

For the C_3(b) cluster (the most stable C_3 cluster proposed by Kalibaeva[9]), both of the two terminal carbon atoms adsorb on the fcc sites, while the middle carbon occupies the hcp site between them. It should be noted that the middle carbon atom only bonds to one of the three nickel atoms on the hcp site (Figure 4). The C−C distances of C_3(b) are 1.322 and 1.325 Å, respectively. The E_{ads}(C) of the C_3(b) cluster is −7.01 eV.

For the C_3(c) cluster, the two terminal carbons adsorb on the fcc and the hcp sites, respectively. The middle carbon atom adsorbs on the bridge site of the Ni(111) surface. The C−C distances of C_3(c) are 1.316 and 1.322 Å, respectively. The E_{ads}(C) of the C_3(c) cluster is −6.80 eV. We also tried the structures of the three-membered ring, but they changed into linear structures during the geometrical optimization.

It is noteworthy that C_3(a) is the most stable structure, while C_3(b) and C_3(c) are higher in energy by 0.40 and 1.02 eV, respectively. This disagrees with Kalibaeva et al.'s result. In their paper, they did not obtain the structure of C_3(a), and reckoned C_3(b) as the most favorable structure.

Four types of stable C_4 clusters were found by calculating many initial structures. C_4(a) has a linear structure formed by adding the fourth carbon atom to C_3(a). The C−C distances of C_4(a) are 1.338, 1.324, and 1.326 Å, respectively, and the E_{ads}(C) is −6.85 eV. For the second type of C_4 cluster, we calculated two possible structures, C_4(b1) and C_4(b2), in order to check the error caused by neglecting the difference between the hcp and fcc sites. In C_4(b1), the three terminal carbon atoms occupy the hcp sites, while the middle carbon occupies the central top site. Comparatively, the three terminal carbon atoms in C_4(b2) occupy the fcc sites. C_4(b1) and C_4(b2) occupy the triangular

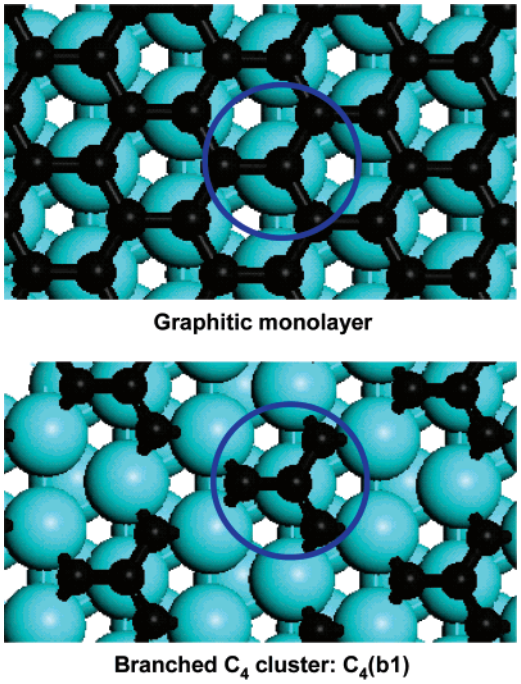

Figure 5. Comparison of the structures of the adsorbed graphitic monolayer and the branched C_4 cluster on the Ni(111) surface.

sites on the Ni(111) surface. The same E_{ads}(C) was found for these two structures. The C−C distances of C_4(b1) and C_4(b2) are longer than those in C_4(a).

As shown in Figure 4, C_4(c) adsorbs on another type of triangular site. Three terminal carbon atoms occupy the hcp sites, while the middle carbon occupies the central fcc site. For C_4-(d), the initial structure was a four-membered ring, but it changes into rhombic structure formed by two three-membered rings during the geometrical optimization. C_4(c) and C_4(d) have relatively less negative E_{ads}(C) (−6.68 and −6.27 eV), respectively.

As given in Table 2, the difference of the E_{ads}(C) between C_4(a) and C_4(b) is only 0.03 eV, indicating their similar stability. Comparatively, the value of C_4(c) is less stable by 0.17 eV, and C_4(d) has the least stability over the four types of C_4 clusters (by 0.58 eV). It shows clearly that the formation of carbon clusters on the Ni(111) surface is more favored than that of the adsorbed carbon atoms and reconstructed structures, by comparing the computed E_{ads}(C).

It is interesting to compare our results with those of Kalibaeva et al.,[9] since very different conclusions were proposed respectively. They calculated the structures of C, C_2, and C_3 clusters on the Ni(111) surface and found that the stable structures are those with the carbon atoms binding to the 3-fold hollow sites. They found that the adsorption sites for carbon atoms differ from those of small clusters and graphite monolayers, i.e., the on-top positions are clearly unfavorable for small carbon clusters; they become favorable in the case of a graphite monolayer. Therefore, they concluded that the mechanism of formation of the graphite monolayer from dispersed atoms must be complex, probably with a significant barrier (for example, the tortuous shape of intermediate size clusters).

In our paper, however, the C_1−C_4 small clusters were calculated and more stable structures were found. For the adsorbed C and C_2 cluster, the carbon atoms bind to 3-fold hollow sites, while the middle carbon atoms in C_3 and branched C_4 clusters bind to the top sites of Ni(111). As shown by the circles in Figure 5, the branched C_4 cluster has already been at the same site as that of the adsorbed graphitic monolayer. Therefore, the mechanism of the formation of the graphite monolayer from branched C_4 cluster should not be complex, and the tortuous shape of intermediate size clusters forecasted by Kalibaeva et al.[9] would not exist in the key pathway of graphitic monolayer formation on Ni(111).

The effects of the size of the unit cell (surface coverage) to the lateral relaxation of the adsorbed small clusters have been tested by the p(3 × 3) unit cell models, as listed in Table 3. The calculation parameters were set to be the same as those for the p(2 × 2) unit cell models. The computed C−C bond lengths by the p(3 × 3) models are a little longer than those by the p(2 × 2) models. The computed E_{ads}(C) by the p(3 × 3) models are less negative than those by the p(2 × 2) models, i.e., the carbon clusters at the lower coverage are more stable than those at the higher coverage. It means the carbon clusters prefer moving close to each other, which could be a factor promoting their aggregation.

3.3. Graphitic Monolayer, Carbon Chain, and Carbon in Ni Bulk. The adsorbed graphitic monolayer, carbon chain, and/or carbon in Ni bulk were calculated to clarify their structures and stability.

The optimized structure of the adsorbed graphitic monolayer is shown in Figure 6, and the E_{ads}(C) is listed in Table 4. For the adsorbed graphitic monolayer, half of the carbon atoms bind with the Ni atoms on the top sites of the Ni(111) surface, while half of them do not. The E_{ads}(C) of graphitic carbon is −7.95 eV. For comparison, we have also computed the adsorption energy corresponding to graphitic sheet, and the computed E_{ads}(C) of graphite is −0.43 eV. It shows that graphitic monolayer adsorption is also favorable thermodynamically. There are two C−C distances for the adsorbed graphitic monolayer on the Ni(111) surface, 1.445 and 1.448 Å, which are longer than that in the free graphitic monolayer (1.410 Å). The graphitic monolayer desorbs from the Ni(111) surface if the carbon atoms of the graphitic monolayer are placed on the 3-fold hollow (fcc and hcp) sites. Therefore, such a structure is unstable. Kalibaeva et al.[9] found that such a configuration could exist, but barely be stable, only when van der Waals terms are included in their calculation. However, we disagree with Rosei et al.'s conclusion that all carbon atoms adsorb on 3-fold hollow sites.[20,21] During the calculation on the small clusters, it was found that the middle carbon prefers to adsorb on top site. This rule is also applicable to the graphitic carbon.

For the adsorbed carbon chains, two stable structures were found. The optimized structures are shown in Figure 7, and the

TABLE 3: Effect of Unit Cell on the Lateral Relaxation of the Small Carbon Clusters, the E_{ads}(C) in eV, and the d_{C-C} in Å

	in p(2 × 2) cell			in p(3 × 3) cell		
species	coverage (ML)	E_{ads}(C)	d_{C-C}	coverage (ML)	E_{ads}(C)	d_{C-C}
C (hcp)	1/4	−7.09		1/9	−6.71	
C_2	1/2	−7.13	1.312	2/9	−7.02	1.322
C_3(a)	3/4	−7.14	1.325/1.325	1/3	−6.97	1.342/1.346
C_4(b2)	1	−6.85	1.428/1.431/1.433	4/9	−6.84	1.457/1.458/1.458

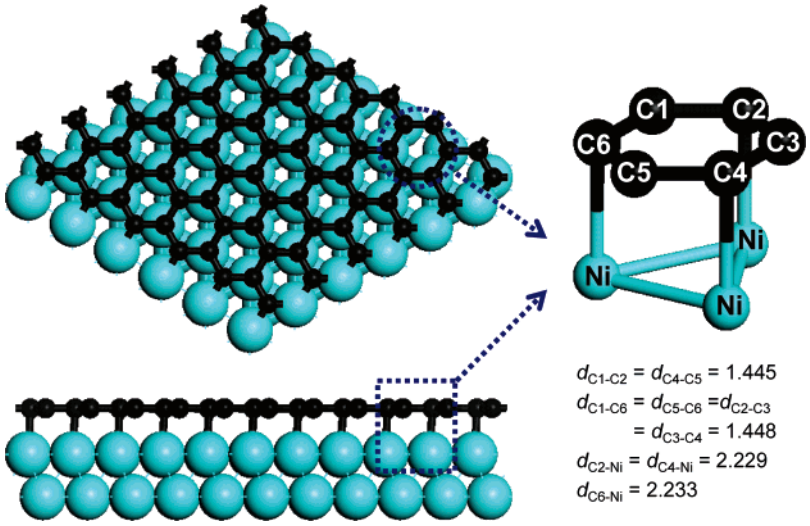

Figure 6. Structure of the adsorbed graphitic monolayer on the Ni(111) surface.

TABLE 4: E_{ads} and the Average E_{ads}(C) of the Adsorbed Graphitic and Chain Carbons and the Carbon in the Ni Bulk

species	no.[a]	E_{ads}	E_{ads}(C)
graphitic C	8	−63.61[b]	−7.95[b]
chain (a)	4	−28.94	−7.23
chain (b)	6	−39.06	−6.51
C (bulk)	1	−7.66	−7.66
C (2bulk)	2	−14.52	−7.26

[a] The number of carbon atoms per p(2 × 2) unit cell. [b] The E_{ads} relative to the graphitic monolayer adsorption is −3.44 eV; the average E_{ads}(C) is −0.43 eV.

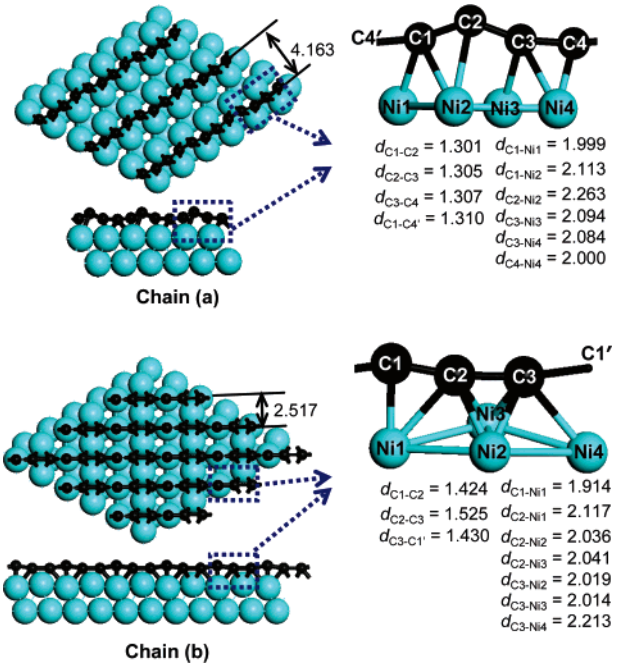

Figure 7. Structures of the adsorbed carbon chains on the Ni(111) surface.

computed adsorption energies are listed in Table 4. The structure of chain 'a' corresponds to the coverage of 1 ML, and four carbon atoms were put into a p(2 × 2) unit cell. In chain 'a', one carbon atom adsorbs on the top site with the C−Ni bond inclined to the Ni(111) surface, while the other three carbon atoms adsorb on the bridge site. The distance between the two parallel adsorbed carbon chains is 4.163 Å, and the computed E_{ads}(C) is −7.23 eV. In chain 'a', the C−C distances are in region of 1.301∼1.310 Å.

The structure of chain 'b' corresponds to 1.5 ML coverage, and six carbon atoms were put into a p(2 × 2) unit cell. In this structure, two carbon atoms adsorb on the top sites, two carbon atoms adsorb on the hcp sites, and the other two adsorb on the fcc sites. The distance between two parallel adsorbed carbon chains is 2.517 Å, which is shorter than that of Fil(a). It indicates that a stronger lateral interaction between the carbon chains exists in the chain 'b' model. In chain 'b', the C−C distances (1.424, 1.430, and 1.450 Å) are longer than those in chain 'a'. The computed E_{ads}(C) (−6.51 eV) of chain 'b' is less negative than that of chain 'a'. Thus, chain 'a' is more stable than chain 'b'.

The carbon in Ni bulk was calculated at the low coverage (0.25 ML) to cast light on the initial stage of carbon sinking. As shown in Figure 8, the carbon atom was located in one of the fcc sites between the top and the second layers. The computed E_{ads}(C) of C (bulk) is −7.66 eV, which is more negative than those of the adsorbed atomic carbon and carbon clusters but less than that of the graphitic monolayer. The C−Ni distances in the C in Ni bulk are shorter than those in the adsorbed graphitic monolayer and the carbon chains. At 0.5 ML, the computed E_{ads}(C) of C (2bulk) is −7.26 eV, and the C−Ni distances are longer than those of 0.25 ML. The two carbon atoms were located in the fcc sites between the top and the second layers.

Carbon sinking into the bulk of Ni crystal plays an important role for catalyst deactivation in many reactions over Ni catalysts.[4,22−24] The adsorbed carbon atoms, produced by adsorbed hydrocarbon or carbon monoxide dissociating, are dissolved in the metal particle. The dissolved carbon diffuses through the particle and nucleates into the fiber at the rear interface. The nickel crystal changes shape into a pear-like particle, leaving small fragments of nickel behind in the whisker.[23]

By comparing the computed E_{ads}(C), the order of the stability of the various carbons on Ni(111) is graphitic monolayer > C in Ni bulk > carbon chain > small cluster > atomic carbon. Thus, the adsorbed graphitic monolayer is the most favored to form on the Ni(111) surface thermodynamically. This sounds different than Kalibaeva's conclusion[9] that the stable state of the nickel/carbon surface is found to be either a clean nickel surface or a fully carbon-covered nickel surface with a graphitic configuration. Their conclusion is applicable when comparing

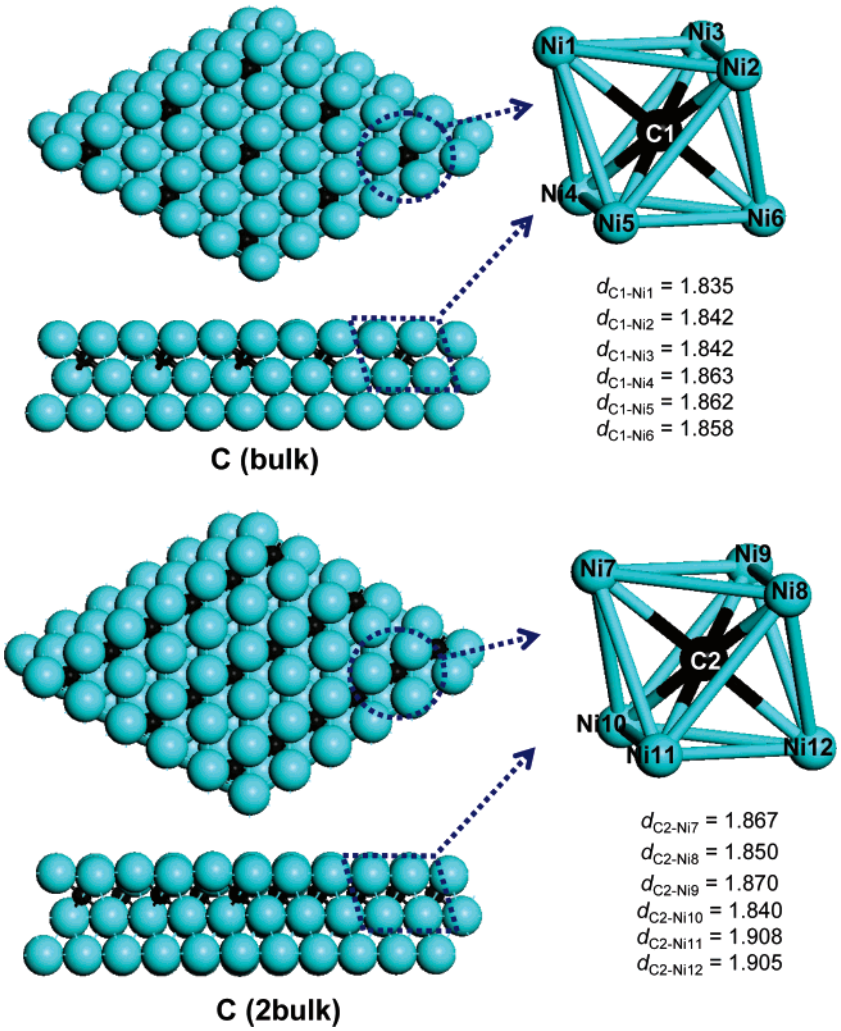

Figure 8. Structures of the adsorbed atomic carbons in the nickel bulk.

the stability of the surfaces without considering the reaction circumstance. The formula (1) in ref 9 does not reflect the situation of C adsorption/desorption. In this study, however, we hope to provide some information of the reaction systems including the C/Ni(111) adsorption/desorption process. The different definitions are applicable for different processes. This is the reason for the adsorption energies employed in our work.

3.4. Energy Barriers of Carbon Transfer. The energy barriers of carbon transfer were calculated to analyze the microkinetic properties of the initial stage of the carbon growth. Both the lateral transfer on the surface and vertical transfer into the Ni bulk were considered at the coverages of 0.25 and 0.5 ML. The potential energy surface at 0.25 ML was shown in Figure 9. The TS graphs in the present paper are only the fit of the three points, and not a complete minimum energy path.

In Figure 9, the energy of C (fcc) was set to zero. The relative energies of C (hcp) and C (bulk) are −0.03 and −0.60 eV, respectively. However, the energy barrier (TS1) of the lateral transfer between C (fcc) and C (hcp) is only 0.50 eV (0.53 eV for the back reaction), while C (fcc) vertical transfer into C (bulk) has the barrier of 1.83 eV (TS2, forward) and 2.43 eV (backward). Therefore, although the carbon in Ni bulk is lower in energy, its formation has a high energy barrier, while the carbon lateral transfer is relatively easier.

At the coverage of 0.5 ML, two carbon atoms were put in a p(2 × 2) cell. After the first step of the vertical transfer, one of them locates in the Ni bulk and another one adsorbs on the Ni(111) surface. The optimized structures of the coexisted in-bulk and on-surface carbon atoms are shown in Figure 10, and the PES of the carbon transfers at 0.5 ML are shown in Figure 11.

Four coexisted modes were obtained for the in-bulk and on-surface carbons, as shown in Figure 10. In C (bs-1), the carbon in Ni bulk locates below a fcc site, and the surface carbon adsorbs over the same fcc site. The computed average E_{ads}(C) of the C (bs-1) is −6.67 eV. The C (bs-2) structure forms after the carbon atom on the fcc site of C (fcc + hcp) sinks into Ni bulk. As mentioned above, in C (fcc + hcp), the two carbon atoms in the p(2 × 2) cell adsorb on a fcc and a hcp site, respectively. The computed average E_{ads}(C) of the C (bs-2) is −6.90 eV. Similarly, the C (bs-3) structure forms after one of the carbon atoms of C (2fcc) sinks into Ni bulk. The computed average E_{ads}(C) of the C (bs-3) is −7.20 eV, which is the most negative in the coexisted structures. Another coexisted structure is C (bs-4), in which the surface carbon adsorbs on the hcp site neighboring to the in-bulk carbon atom. The computed average E_{ads}(C) of C (bs-4) is −7.00 eV.

In Figure 11, the energy of C (fcc + hcp) was set to zero, and the relative energies of the intermediates and the energy barriers of the elementary steps were also labeled. The difference between the relative energies of C (fcc + hcp) and C (2fcc) is 0.03 eV, while the energy barrier of the transfer between them is 0.61/0.64 eV (TS6). The barrier for C_2 cluster formation from C (2fcc) is 0.36 eV (TS3). The low barrier indicates that the

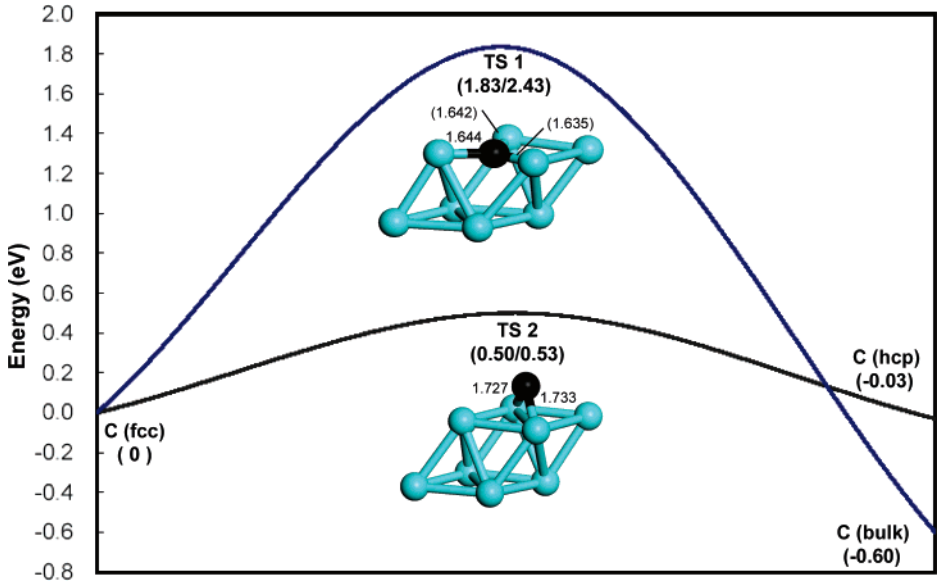

Figure 9. PES of the carbon transfers on the Ni(111) surface at the coverage of 0.25 ML.

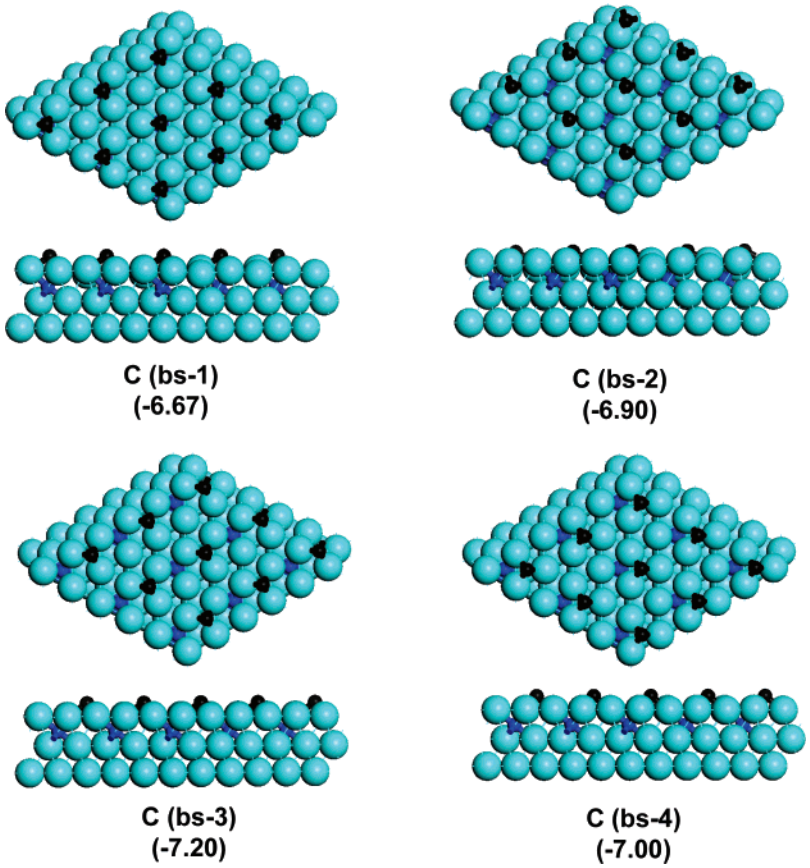

Figure 10. Structures of the coexisted in-bulk (blue) and on-surface (black) carbon atoms and their average E_{ads}(C) (eV).

transformation between C (fcc + hcp) and C (2fcc) is feasible, and the formation of the C_2 cluster from atomic carbon is favorable.

The energy barriers of the carbon vertical transfer at 0.5 ML were calculated for comparison. The C (fcc + hcp) transfer into C (bs-2) has an energy barrier of 1.86 eV (TS7), while that of C (2fcc) to C (bs-3) is 1.23 eV (TS4). The energy barrier for the transfer between C (bs-2) and C (bs-3) is 0.19/0.78 eV. Moreover, the formation of C (2bulk) by another surface carbon of C (bs-3) transferring into Ni bulk has an energy barrier of 1.64 eV. The high energy barriers indicate that the vertical transfer of carbon at 0.5 ML is also difficult, although the structures of the carbon in Ni bulk are thermodynamically stable.

Therefore, the carbon lateral transfer and aggregation are favored kinetically. Moreover, the formation of graphitic monolayer is most favored thermodynamically, followed by the carbon in Ni bulk.

3.5. Electronic Property. The charges and the spin densities of the C_n/Ni(111) complexes were calculated, and the results are listed in Table 5. The total spin densities of four Ni atoms on the first layer of clean Ni(111) are 3.36, while the total net charges of them are −0.20 e.

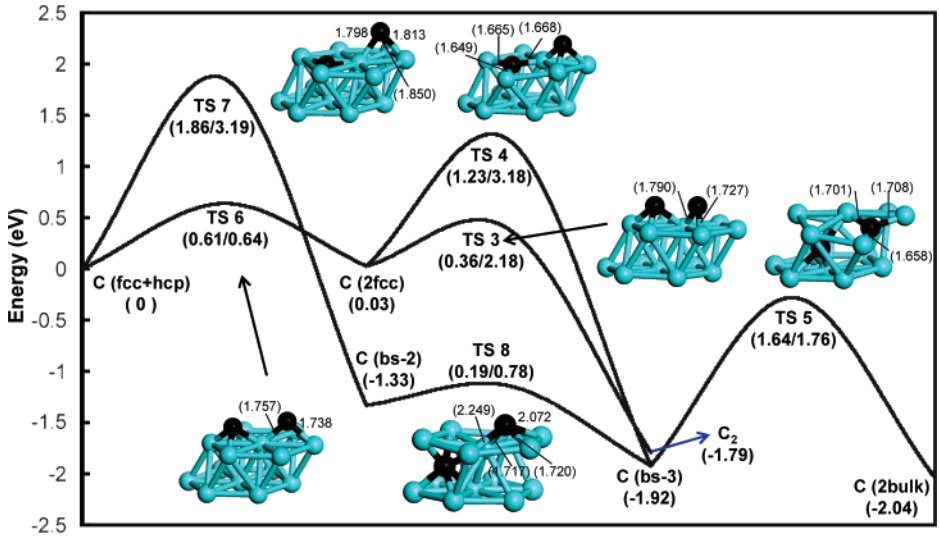

Figure 11. PES of the carbon transfers on the Ni(111) surface at the coverage of 0.5 ML.

TABLE 5: Total Charges (*q*, e) and Spin Densities (*S*) of the Four Ni Atoms on the First Layer of the Ni(111) Surface, as Well as Those of the Adsorbed Carbon Species

species	coverage (ML)	q_{Ni}	S_{Ni}	q_C	S_C
Ni(111)		−0.20	3.36		
C (fcc)	0.25	0.31	0.92	−0.43	−0.04
C (hcp)	0.25	0.35	0.96	−0.45	−0.04
C (fcc+hcp)	0.5	0.65	0.62	−0.78	0.18
C (2fcc)	0.5	0.57	0.14	−0.68	0.12
R(a)	0.75	1.14	0.78	−1.23	0.06
R(b)	1	1.21	0.04	−1.27	−0.08
C_2	0.5	0.75	2.12	−0.87	0.28
C_3(a)	0.75	1.02	1.22	−1.11	0.08
C_4(a)	1	1.27	1.34	−1.32	0.16
graphitic C	2	0.92	2.00	−0.88	0
chain (a)	1	1.11	1.40	−1.18	0.04
chain (b)	1.5	1.74	0.20	−1.68	−0.04
C (bulk)	0.25	0.12	0.52	−0.58	−0.04
C (2bulk)	0.5	0.44	0	−1.16	0

The spin densities of the first-layer Ni atoms decrease in different degrees by carbon species adsorption. For the atomic carbon species C (fcc) and C (hcp), three-fourths of the Ni atoms bind with the adsorbed carbon atoms at 0.25 ML, and the spin densities of the Ni atoms on the first layer reduce from 3.36 to 0.92 and 0.96, respectively. At 0.5 ML, the spin densities are lower than those of 0.25 ML. The net charge of the Ni atoms on the first layer changed to positive after adsorption of atomic carbon species. At the same time, the adsorbed atomic carbon species are negatively charged, indicating electron transfer from the Ni(111) surface to atomic carbon species during adsorption.

At 0.75 ML, the Ni(111) surface reconstructs due to the adsorption of carbon atoms. The spin density of the drawn-out Ni atom reduces to 0.06, while those of the other first-layer Ni atoms only reduce to 0.24. As a consequence, the spin densities of the four first-layer Ni atoms are 0.78. At 1 ML, the spin density of the first-layer Ni atoms of the reconstructed structure is reduced to 0.04.

The spin densities of C_2 and C_4(a) are reduced to 0.28 and 0.16, respectively. It is noteworthy that the C_2 and C_4(a) cluster also have spin electrons after adsorption. One of the terminal carbons has a spin electron in adsorbed C_4(a). These two clusters remain partial spin densities, respectively. The resemblance of the two structures is that the carbon atom neighboring the terminal carbon adsorbs on a 3-fold hollow site.

For the graphitic monolayer on the Ni(111), the spin density of the first-layer Ni atoms is 2.00, which is the largest in the computed carbon species/Ni(111) complexes. Those of chain 'a' and chain 'b' are 1.40 and 0.20, respectively. For the carbon in Ni bulk, the spin density of the first layer Ni atoms is 0.52.

Apparent charge transfer was found between the Ni(111) surface and the adsorbed carbon species, as shown in Table 5. After the adsorption of the carbon species, the first-layer Ni atoms of the Ni(111) surface have the positive charges of 0.31∼1.74 e, while the adsorbed carbon species have the negative charge of −0.43 ∼ −1.68 e. Therefore, electrons transfer from the Ni(111) surfaces to the adsorbed carbon species, and as a consequence the spin densities of both the adsorbed carbon species and the Ni surface decrease during the adsorption processes.

4. Conclusion

A set of states of adsorbed carbons on Ni(111) was computed by using density functional theory. By comparing the computed adsorption energies, the stability of these carbons on Ni(111) is in the following order: graphitic monolayer > C in Ni bulk > carbon chain > small cluster > atomic carbon. The adsorbed graphitic monolayer is the most preferred to form on Ni(111) thermodynamically.

The adsorbed atomic carbon is the least stable on one hand, and the most active on the other. It was found that the adsorbed carbon atoms exist at coverage lower than 0.5 ML, while the dispersed carbon atoms at 0.75 and 1 ML induce the reconstruction of the Ni(111) surfaces and the formation of the net structures including Ni_3 and Ni_3C_6 rings. This implies that we could synthesize the net structure by self-assembly if we can prepare the dispersed carbon atoms at the coverage of 0.75 and 1 ML on the Ni(111) surfaces.

For the adsorbed small carbon clusters on Ni(111), the terminal carbons prefer occupying 3-fold hollow sites. Two atoms of the C_2 cluster adsorb on fcc and hcp sites, respectively. The middle carbon atom in the C_3 cluster occupies a top site, while the two middle carbon atoms in the linear C_4 structure occupy a top and a 3-fold hollow site (hcp or fcc), respectively. The stable branched C_4 structures have stabilities comparative to the linear C_4 structure, and the middle carbon atom of the stable branched C_4 structure prefers adsorbing on the top site of the Ni(111) surface.

After the small carbon clusters grow to the carbon deposition, the graphitic monolayer has relatively lower energy than the carbon chain. For the adsorbed graphitic monolayer, half of the carbon atoms bind with Ni atoms on top sites, while half of them are located over, but did not bind with, the 3-fold hollow sites (hcp and fcc).

By comparing the stable structures of the adsorbed small carbon clusters and the adsorbed graphitic monolayer, the mechanism of the formation of the graphite monolayer from the branched C_4 cluster should not be a complex one, and the tortuous shape of intermediate size clusters forecasted by Kalibaeva[9] would not exist in the key pathway of graphitic monolayer formation on Ni(111).

Unlike the above carbon species, the carbon atom in Ni bulk does not cover the Ni surface; however, it apparently reduces the spin density and changes the partial density of states of the first Ni layer.

The energy barriers of the lateral and vertical transfers were obtained by calculating the transition states. The lateral transfer and the aggregation of the surface carbons were favored with very low energy barriers. On the contrary, the vertical transfer of carbon atoms into the Ni bulk has very high energy barriers. It indicates that the formation of the carbon in Ni bulk is a thermodynamic process, and the lateral transfer is a kinetic process.

These adsorbed carbon species change the electron properties in different degrees. During the adsorption processes, electrons transfer from the Ni surfaces to the adsorbed carbon species, and the spin densities of both the adsorbed carbon species and the Ni surface decrease.

Acknowledgment. This work was supported by the Chinese Academy of Sciences and the National Natural Science Foundation of China (Nos. 20473111 and 20590361) and the National Outstanding Young Scientists Foundation of China (No. 20625620).

References and Notes

(1) Zhang, Z. L.; Verykios, X. E. *Catal. Today* **1994**, *21*, 589.

(2) Hu, Y. H.; Ruckenstein, E. *Adv. Catal.* **2004**, *48*, 297.

(3) Schouten, S. C.; Gijzeman, O. L. J.; Bootsma, G. A. *Bull. Soc. Chim. Belg.* **1979**, *88*, 541.

(4) Bartholomew, C. H. *Catal. Rev. Sci. Eng.* **1982**, *24*, 67.

(5) Ginsburg, J. M.; Pina, J.; Solh, T. E.; de Lasa, H. I. *Ind. Eng. Chem. Res.* **2005**, *44*, 4846.

(6) Rostrup-Nielsen, J. R.; Trimm, D. L. *J. Catal.* **1977**, *48*, 155.

(7) Rostrup-Nielsen, J. R. *Catal. Today* **1997**, *37*, 225.

(8) Bartholonew, C. H. *Appl. Catal., A* **2001**, *212*, 17.

(9) Kalibaeva, G.; Vuilleumeir, R.; Meloni, S.; Alavi, A.; Ciecotti, G.; Rosei, R. *J. Phys. Chem. B* **2006**, *110*, 3638.

(10) (a) Payne, M. C.; Allan, D. C.; Arias, T. A.; Joannopoulos, J. D. *Rev. Mod. Phys.* **1992**, *64*, 1045. (b) Milman, V.; Winkler, B.; White, J. A.; Pickard, C. J.; Payne, M. C.; Akhmataskaya, E. V.; Nobes, R. H. *Int. J. Quantum Chem.* **2000**, *77*, 895.

(11) (a) Perdew, J. P.; Zunger, A. *Phys. Rev. B* **1981**, *23*, 5048. (b) Perdew, J. P.; Chevary, J. A.; Vosko, S. H.; Jackson, K. A.; Pederson, M. R.; Singh, D. J.; Fiolhais, C. *Phys. Rev. B* **1992**, *46*, 6671.

(12) Vanderbilt, D. *Phys. Rev. B* **1990**, *41*, 7892.

(13) Monkhorst, H. J.; Pack, J. D. *Phys. Rev. B* **1976**, *13*, 5188.

(14) Wang, S.-G.; Cao, D.-B.; Li, Y.-W.; Wang, J.; Jiao, H. *J. Phys. Chem. B* **2005**, *109*, 18956.

(15) Wang, S.-G.; Cao, D.-B.; Li, Y.-W.; Wang, J.; Jiao, H. *Surf. Sci.* **2006**, *600*, 3226.

(16) Bengaard, H. S.; Alstrup, I.; Chorkendorff, I.; Ullmann, S.; Rostrup-Nielsen, J. R.; Nørskov, J. K. *J. Catal.* **1999**, *187*, 238.

(17) Ciobîcă, I. M.; Frechard, F.; van Santen, R. A.; Kleyn, A. W.; Hafner, J. *J. Phys. Chem. B* **2000**, *104*, 3364.

(18) Ledentu, V.; Dong, W.; Sautet, P. *J. Am. Chem. Soc.* **2000**, *122*, 1796.

(19) Halgren, T. A.; Lipscomb, W. N. *Chem. Phys. Lett.* **1977**, *49*, 225.

(20) Rosei, R.; De Crescenzi, M.; Sette, F.; Quaresima, C.; Savoia, A.; Perfetti, P. *Phys. Rev. B* **1983**, *28*, 1161.

(21) Rosei, R.; Modesti, S.; Sette, F.; Quaresima, C.; Savoia, A.; Perfetti, P. *Phys. Rev. B* **1984**, *29*, 3416.

(22) Nørskov, J. K.; *Adv. Catal.* **2002**, *47*, 65.

(23) Rostrup-Nielsen, J. R. In *Catalysis, Science and Technology*; Anderson, J. R., Boudart, M., Eds; Spinger: Berlin, 1984, Vol. 5, Chapter 1.

(24) Eizenberg, M.; Blakely, J. M. *Surf. Sci.* **1979**, *82*, 228.